Surface Science 718 (2022) 122006

Contents lists available at ScienceDirect

Surface Science

journal homepage: www.elsevier.com/locate/susc

A magnetic map of O/Fe/Mn/Fe(001) multilayer with DFT+U scheme

J.C. Avila-Gaxiola [a], J.G. Ibarra-Armenta [b], R.E. Félix-Medina [b], S. Meza-Aguilar [*,b], C. Demangeat [c]

[a] Facultad de Ciencias de la Tierra y el Espacio de la Universidad Autónoma de Sinaloa, Av. Las Americas y Blvd. Universitarios, Colonia Universitaria, C. P. 80010, Culiacán Sinaloa, México

[b] Facultad de Ciencias Físico-Matemáticas, Universidad Autónoma de Sinaloa, Calzada de las Américas y Universitarios, Colonia Universitaria, C.P. 80010, Culiacán Sinaloa, México

[c] UFR de Physique et d'Ingénierie, 3 rue de l'Université, Strasbourg 67000, France

ARTICLE INFO

Keywords:
Mn oxide
Magnetic thin films
Density-functional calculations
Ultrathin transition metal oxide

PACS:
75.75.-c
75.75.Lf
75.70.-i

ABSTRACT

Zenia et al. (Surface Science 584 (2005) 146152) have shown that a Mn monolayer on Fe(001) is in-plane antiferromagnetic. They have also obtained a ferromagnetic as well as an antiferromagnetic coupling between Mn and Fe in the subsurface layer but those couplings are found higher in energy. When an oxygen monolayer is added this in-plane antiferromagnetic solution becomes unstable. Besides Meza-Aguilar and Demangeat (Eur. Phys. J. B 93 (2020) 107 have shown that the interlayer exchange coupling in Fe/Cr/Fe(001) can be modified by the inclusion of one monolayer of oxygen i.e. O/Fe/Cr/Fe(001). In the present communication, we study the magnetic stability of a Mn monolayer on Fe(001) and the interlayer exchange coupling in Fe/O/Mn/Fe(001) and O/Fe/Mn/Fe(001) multilayers with a DFT+U scheme. The Fe/O/Mn/Fe(001) multilayer is energetically clearly unstable and convergency leads to the displacement of the oxygen monolayer on top of the Fe surface atoms so that we restrict ourselves to the determination of the magnetic map of O/Fe/Mn/Fe(001). The interlayer exchange coupling in Fe/Mn/Fe(001) is modified by adding a monolayer of oxygen atoms on it. This is very similar to the result obtained recently on Fe/Cr/Fe(001) multilayers.

1. Introduction

The oxidation of Fe remains nowadays a study of current interest[1] (and references therein). Also oxidation of more complex substrates like antiferromagnetic layers on ferromagnet were investigated. For example Yonamoto[2] *et al* have studied the effect of oxygen on Mn/Co(001) by XMCD. They found that magnetic coupling between Mn and Co is ferromagnetic for low oxygen coverage but it changes to antiferromagnetic for the high coverage. Later on Tange[3] *et al* have studied the deposition of Mn monolayer on FeO, they found that the oxygen enhances the spin polarization of Mn, but the antiferromagnetic coupling between Mn and Fe does not change when oxygen is grown on Mn/Fe surface. More recently Picone[4] *et al* and Calloni[5] *et al* have probed CrO on Fe(001), using angle- and spin-resolved photoemission spectroscopy, low-energy electron diffraction, and scanning tunneling spectroscopy with ab initio calculations, and they found that in the submonolayer regime a novel $c(4\times 2)$ overlayer self-assembles on the Fe(001)-$p(1\times 1)$ O surface, saturating for a coverage of about 0.75 monolayers. This phase becomes unstable for higher coverages, when a $(\sqrt{5}\times\sqrt{5})R27^0$ superstructure emerges for submonolayer regime.

The properties of ultrathin magnetic films are of particular importance, in studies from experimental and theoretical point of view. These systems show novel magnetic and electronic features due to reduced dimensions, compared with bulk systems. Demangeat and Parlebas [6] have reported on manganese nanostructures which have been the subject of a number of investigations because manganese is a unique element which exhibits a variety of unusual electronic and magnetic properties depending on its environment. Ernst *et al.* [7] have investigated the electronic and magnetic structures of Mn films with thickness of up to 12 monolayers on Fe(001) by means of first principles calculations. The magnetic moment at the Mn surface and at the Mn-Fe interface are significantly enhanced, as compared to the respective bulk values.

Zenia *et al.* [8] have studied the effect of oxidation of a Mn monolayer deposited on Fe(001) to which a top layer of O is added. The most important effect of the oxygen is the stabilization of the $p(1\times 1)$

---

[*] Corresponding author.
E-mail address: smeza@uas.edu.mx (S. Meza-Aguilar).

https://doi.org/10.1016/j.susc.2021.122006
Received 21 June 2021; Received in revised form 6 December 2021; Accepted 9 December 2021

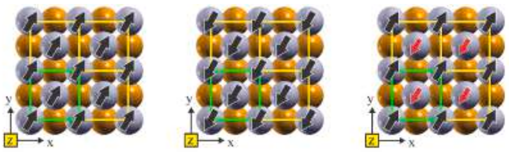

a) p(1x1)↑ b) p(1x1)↓ c) c(2x2)

Fig. 1. Input magnetic configurations for Mn/Fe(001). ↑ (↓) represent a ferromagnetic (antiferromagnetic) coupling between Mn atoms and Fe substrate atoms. The grey (orange) spheres represent the Mn surface atoms (Fe substrate) atoms. The green line is the unit cell in plane. For the Mn/Fe(001) bcc the IMC are a) p(1 × 1)↑, b) p(1 × 1)↓ and c) c(2 × 2). (For interpretation of the references to colour in this figure legend, the reader is referred to the web version of this article.)

ferromagnetic solution at the expense of the previously strongly stable $c(2 \times 2)$ configuration, with a difference in energy between these two solutions of 30.6 meV/Mn atom. Pick *et al.* [9] have studied the oxidation of the interface Mn-Co/Co(001) fcc using first principles calculations. They found that the Mn and Co atoms are coupled ferromagnetically, and deposition of oxygen enhances the stability. Very recently, Meza-Aguilar and Demangeat [10] have studied the oxygen atoms deposited on Fe/Cr/Fe(001) using first principles calculations. They have explained that the effect of the oxygen adsorbed layer is to alter strongly the local density of states on the Fe atoms and this can explain the modification of the interlayer exchange coupling (IEC).

In the present communication we intend to discuss the effect of oxygen on the IEC in Fe/Mn multilayers. Section 2 is devoted to a short description of the method used whereas Section 3 presents the results obtained. First we start by confirming the IEC in Fe/Mn/Fe(001) multilayered systems. Then we successively perform calculations on Fe/O/Mn/Fe(001) with DFT and DFT + U codes in order to point out that those systems are energetically unstable and that O tends to move on top of the Fe atomic layer. Finally we perform calculations by starting with the O/Fe/Mn/Fe(001) configuration in order to display the drastic effect of O on the IEC of Fe/Mn multilayers. Section 4 is devoted to the conclusion.

2. Computational details

The ground state of iron substrate is obtained through density functional theory (DFT[11]). However, the MnO adlayers cannot be satisfactorily described by this DFT only method. A good approach to find the ground state of this oxide is DFT + U proposed by Anisimov *et al.* [12] and Liechtenstein *et al.* [13] The MnO ultrathin films are therefore described by the DFT + U method with the following approximations: 1) U = 3.0 eV for Fe and Mn [14]; 2) this value is used for Mn and Fe atoms at nearest neighboring positions to the O atom; 3) for the other Fe atoms the value of U = 0 is used. In the present work, we have used the Quantum-Espresso code[15], which is based on the DFT. We have used the Generalized Gradient Approximation of Perdew-Burke-Ernzerhof (GGA-PBE)[16]. The pseudopotentials used were taken from the Quantum Espresso Distribution [17] with scalar relativistic calculations, with exchange-correlation of Perdew-Burke-Ernzerhof [16], with ultrasoft pseudopotentail Vanderbilt [18] for the three atoms. The Fe, Mn and O, pseudopotential files were obtained by using the electronic configuration for each atom $[Ar]3d^64s^2$, $[Ar]3d^54s^2$ and $1s^22s^22p^4$, respectively. For Fe and Mn we have considered semi-core state in valence. We have used a cutoff energy of 35 *Ry* for the plane waves expansion of the pseudowave functions (560 *Ry* for the charge density and potential). The Monkhorst-Pack scheme was used to define the $\overrightarrow{k}$ points and the calculations for each cell were performed with a grid of 32 × 32 × 2 mesh [19] in $\overrightarrow{k}$-space. First we have determined the equilibrium positions by relaxing the systems until the total force is less than 0.001 Ryd/Cell. For the calculations we have used a slab geometry with a film of 13 planes of Fe(001) bcc substrate. On both sides of this slab we have added the following multilayers: (1) in contact with the Fe slab we have first added a Mn monolayer and above a Fe monolayer which is now the surface; (2) in between the Fe surface monolayer and the Mn monolayer we add an oxygen monolayer i.e. Fe/O/Mn/Fe(001); (3) finally we have considered a trilayer film on Fe(001) i.e. O/Fe/Mn/Fe(001). Only two inequivalent atoms per plane are considered whereas full relaxation perpendicular to the planes is considered for all layers put on the Fe-slab. Also 2 layers of the Fe-slab are fully relaxed.

Table 1
Difference of total energies ΔE for Mn/Fe(001) with 2 inequivalent atoms per plane. Three magnetic configurations have been considered i.e. a) $p(1 \times 1)\uparrow$, b) $c(2 \times 2)$, c) $p(1 \times 1)\downarrow$. Magnetic moments in μ_B, interlayer distance (d_I in Å) and total energy difference (in meV/atom) respect to the ground state noted by 0. Calculations are performed with DFT-code.

Mn/Fe(001)			
Mn	a)	b)	c)
ΔE	13	0	36
	μ_B/d_I	μ_B/d_I	μ_B/d_I
Mn	3.97/1.57	–4.31/1.47	–4.12/1.46
Mn		3.86/1.55	
Fe_S	2.25/1.41	1.96/1.41	2.17/1.45
Fe_S		1.96/1.41	
Fe_{S-1}	2.31/1.43	2.54/1.43	2.56/1.43
Fe_{S-1}		2.53/1.50	
Fe_{S-2}	2.33/1.43	2.51/1.46	2.43/1.45
Fe_{S-2}		2.51/1.46	

3. Results

First we determine the ground state for Mn/Fe(001) bcc, using three input magnetic configurations $p(1 \times 1)\downarrow$, $p(1 \times 1)\uparrow$ and $c(2 \times 2)$ displayed in Fig. 1. The results obtained are presented in Table 1. We report the magnetic moments (in μ_B), the interlayer distance (d_I^{SA}) and the total

Table 2
Magnetic map and difference of total energy (ΔE in meV/atom), respectively to the ground state noted 0, for Fe/Mn/Fe(001). The input magnetic configurations (IMC) noted a), b), c), d), e), f) and g) are defined in Fig. 2. The magnetic moments on Fe and Mn (in μ_B), the interlayer distance (d_I in Å) and total energy difference (in meV/atom) respect to the ground state noted by 0.0. Calculations are performed with DFT-code.

Fe/Mn/Fe(001)							
IMC	a)	b)	c)	d)	e)	f)	g)
ΔE	32	71	39	49	0	52	6
	μ_B/d_I	μ_B/d_I	μ_B/d_I	μ_B/d_I	μ_B/d_I	μ_B/d_I	μ_B/d_I
Fe	3.16/1.45	2.80/1.57	2.99/1.55	–2.82/1.30	–3.16/1.57	–2.83/1.35	–3.13/1.34
Fe			2.99/1.55			–2.83/1.35	3.02/1.34
Mn	1.69/1.38	–3.24/1.49	–3.48/1.44	2.05/1.52	–2.85/1.44	–1.29/1.46	0.12/1.43
Mn			2.29/1.54			2.22/1.49	–0.12/1.42
Fe_S	1.83/1.43	2.31/1.42	2.31/1.44	2.44/1.42	2.37/1.45	2.42/1.42	2.36/1.43
Fe_S			2.31/1.44			2.42/1.42	2.32/1.42
Fe_{S-1}	2.45/1.44	2.51/1.45	2.53/1.44	2.37/1.46	2.50/1.44	2.47/1.45	2.40/1.45
Fe_{S-1}			2.53/1.47			2.45/1.49	2.41/1.44
Fe_{S-2}	2.44/1.44	2.49/1.45	2.51/1.45	2.47/1.44	2.46/1.46	2.51/1.45	2.44/1.45
Fe_{S-2}			2.51/1.45			2.51/1.45	2.46/1.44

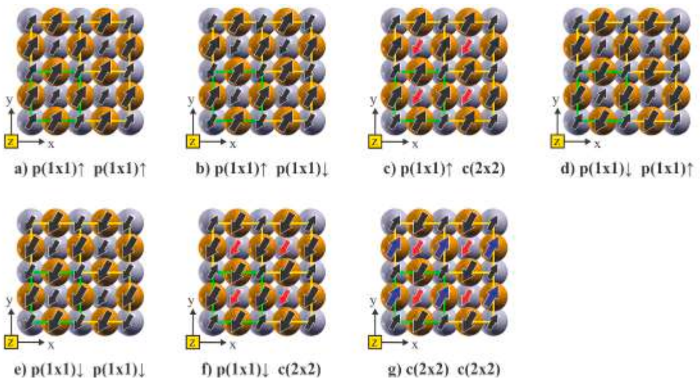

a) p(1x1)↑ p(1x1)↑ b) p(1x1)↑ p(1x1)↓ c) p(1x1)↑ c(2x2) d) p(1x1)↓ p(1x1)↑

e) p(1x1)↓ p(1x1)↓ f) p(1x1)↓ c(2x2) g) c(2x2) c(2x2)

Fig. 2. Input magnetic configurations for Fe/Mn/Fe(001). ↑ (↓) represent a ferromagnetic (antiferromagnetic) coupling between Mn atoms and Fe substrate atoms. The orange (grey) circles represent the Fe surface atoms (Mn subsurface) atoms. The first magnetic configuration corresponds to Fe surface atoms and the second magnetic configuration corresponds to Mn subsurface atoms. The green line is the unit cell in plane.

energy difference between the ground state (noted by 0.0).

The interlayer distance (d_I^{SA} in Å), this distance is defined by the following equation:

$$d_I^{SA} = z^{SA} - \frac{1}{2}\left(z^{(S-1)A} + z^{(S-1)B}\right)$$

where d_I^{SA} is the interlayer distance between A atom localized at S plane, z^{SA} is the z-coordinate for the A atom localized at S-plane and $z^{(S-1)A}$ ($z^{(S-1)B}$) is the z-coordinate for the A (B) atom localized at $S-1$ plane.

For the Fe substrate monolayers we have used the following notation: Fe_S for the Fe atoms in the surface of the substrate, Fe_{S-1} for the Fe atoms in the subsurface of the substrate, Fe_{S-2} for the Fe atoms in the sub-subsurface of substrate, and finally Fe_{S-3} for the Fe atoms in the central monolayer of the slab, but these values are not presented. When there are equivalent magnetic configurations in the same plane or monolayer we present only the results for one of them.

The c(2 × 2) input magnetic configuration is the ground state, in agreement with previous calculation[8]. The first (second) excited state is p(1 × 1)↓ (p(1 × 1)↑) with a difference of total energy with the ground state of 13 (36) meV/atom. The magnetic moments for the ground state are -4.31 μ_B and 3.86 μ_B.

After having reproduced the results for Mn/Fe(001), we have done the calculations for Fe/Mn/Fe(001) with seven input magnetic configurations, displayed in the Fig. 2. In the Fig. 2 the ↑ (↓) is the ferromagnetic (antiferromagnetic) coupling between Fe surface atoms and Fe substrate atoms. The same notations are used for the coupling between Mn subsurface atoms and Fe substrate atoms. The results obtained are presented in Table 2, in which the magnetic moments (in μ_B), the interlayer distance (d_I in Å) and the total energy difference between the ground state (noted by 0). The ground state is for Fe $p(1\times1)\downarrow$ and for Mn $p(1\times1)\downarrow$. In the ground state the magnetic moments for Fe surface (Mn subsurface) atoms are -3.16 μ_B (-2.85 μ_B). The interlayer distances are 1.57 Å and 1.44 Å for the Fe surface monolayer and Mn subsurface monolayer, respectively.

Now we focus on the effect of Oxygen on the stability and magnetic map of Fe/Mn/Fe(001) which is the main part of the present communication. After having determined the magnetic map for Mn/Fe(001) as well as Fe/Mn/Fe(001) we examine the effect of Oxygen on Fe/Mn/Fe (001). The geometrical arrangement is the same as that we have recently considered for Fe/Cr/Fe(001) i. e. a monolayer of Oxygen in between the Fe surface and the Cr subsurface i.e. Fe/O/Cr/Fe(001)[10] and a monolayer of Oxygen adsorbed i.e. O/Fe/Cr/Fe(001). In this paper it was reported that the configuration O/Fe/Cr/Fe(001) was more stable than the Fe/O/Cr/Fe(001) one so that we start here with the O/Fe/Mn/Fe(001). In order to obtain a more complete analysis we have also considered the Fe/O/Mn/Fe(001) multilayers but we have restricted to a few input magnetic configurations.

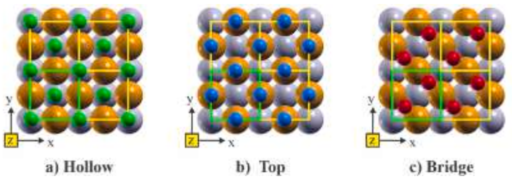

a) Hollow b) Top c) Bridge

Fig. 3. Atomic positions within the unit cell of O/Fe/Mn/Fe(001) with Fe atoms (orange) and Mn atoms (grey). The three oxygen adsorption sites considered are the (a) Hollow (green circles), (b) Top (blue circles) and (c) Bridge (red circles). (For interpretation of the references to colour in this figure legend, the reader is referred to the web version of this article.)

Table 3
Results for O monolayer with different sites of adsorption. The sites are (a) Hollow, (b) Top and (c) Bridge. We present the magnetic moments (in μ_B), the interlayer distances (in Å) and difference of total energy (in meV/atom). Calculations are performed with DFT-code.

O/Fe/Mn/Fe(001)			
IMC	(a) Hollow	(b) Top	(c) Bridge
ΔE	0	284	130
	μ_B/d_I	μ_B/d_I	μ_B/d_I
O	–0.20/0.39	–0.20/1.56	–0.26/1.03
Fe	–3.17/1.58	–1.41/1.46	–2.43/1.74
Mn	–2.17/1.42	–2.66/1.42	–2.88/1.43
Fe_S	2.48/1.44	2.24/1.44	2.43/1.45
Fe_{S-1}	2.51/1.43	2.54/1.43	2.54/1.43
Fe_{S-2}	2.46/1.46	2.45/1.45	2.45/1.45

In order to determine the magnetic map of O/Fe/Mn/Fe(001) we have considered seven input magnetic configurations (IMC) displayed in Fig. 2. In all calculations the oxygen atom is localized at the hollow site. But we have also studied other adsorption sites, the bridge and top site, show in the Fig. 3. The results obtained are shown in the Table 3. Also, we have restricted only one case the e) input magnetic configuration ($p(1\times1)\downarrow$ and $p(1\times1)\downarrow$). The ground state for three adsorption sites is (a) Hollow site. The difference of total energy between the ground state (noted by 0) and the first state is 130 meV/atom (284 meV/atom) for the (c) Bridge site ((b) Top site).

Those IMC for O/Fe/Mn/Fe(001) are indeed the same than those for Fe/Mn/Fe(001) because the addition of an O monolayer does not perturb the IMC because on this O monolayer we choose to put a zero magnetic moment as input. Contrary to the case of Fe/Mn/Fe(001), for the input f) no convergency was obtained. For all other input magnetic configurations convergency was obtained. The results are reported in Table 4. The ground state (noted by 0) is when the Fe subsurface atoms

Table 4
Magnetic map and difference of total energy ΔE (in meV/atom), respectively to the ground state noted 0, for O/Fe/Mn/Fe(001) bcc. The input magnetic configurations (IMC) noted a), b), c), d), e), f) and g) are the same as those reported in Fig. 2 for Fe/Mn/Fe(001). The magnetic moments on Fe and Mn (in μ_B), the interlayer distance (d_I in Å) and total energy difference (in meV/atom) respect to the ground state noted by 0.0. Calculations are performed with DFT-code.

O/Fe/Mn/Fe(001)							
IMC	a)	b)	c)	d)	e)	f)	g)
ΔE	23	53	20	37	0	Non-Conv	37
	μ_B /d_I	μ_B/d_I	μ_B/d_I	μ_B/d_I	μ_B/d_I	μ_B/d_I	μ_B/d_I
O	0.20/ 0.41	0.18/ 0.29	0.20/ 0.36	−0.27/ 0.41	−0.20/ 0.39		−0.02/ 0.45
O			0.23/ 0.36				−0.05/ 0.41
Fe	3.23/ 1.56	3.09/ 1.75	3.24/ 1.71	−3.34/ 1.61	−3.17/ 1.58		−3.38/ 1.63
Fe			3.24/ 1.71				3.21/ 1.48
Mn	1.32/ 1.34	-3.38/ 1.42	2.46/ 1.50	2.87/ 1.51	−2.17/ 1.42		−2.48/ 1.42
Mn			−3.47/ 1.50				0.60/ 1.42
Fe_S	1.77/ 1.43	2.11/ 1.41	2.27/ 1.43	2.38/ 1.42	2.48/ 1.44		2.39/ 1.44
Fe_S			2.27/ 1.43				2.27/ 1.43
Fe_{S-1}	2.44/ 1.45	2.54/ 1.44	2.53/ 1.47	2.39/ 1.45	2.51/ 1.43		2.53/ 1.45
Fe_{S-1}			2.54/ 1.47				2.47/ 1.44
Fe_{S-2}	2.43/ 1.44	2.46/ 1.45	2.51/ 1.46	2.43/ 1.44	2.46/ 1.46		2.49/ 1.46
Fe_{S-2}			2.51/ 1.46				2.48/ 1.46

as well as the Mn atoms are coupled antiferromagnetically with the Fe substrate atoms. The magnetic moments in the ground state, are -0.20 μ_B for O surface atoms, -3.17 μ_B for Fe subsurface atoms and -2.17 μ_B for Mn atoms. The interlayers distances are 0.39, 1.58 and 1.42 Å for the three first monolayer (O, Fe and Mn respectively).

From the 5 metastable magnetic configurations noted a, b, c, d, and g we discuss the solution noted c. This solution presents a $c(2\times2)$ magnetic configuration similar to the c solution obtained (see Table 2) for Fe/Mn/Fe(001) and to the ground state for Mn/Fe(001). It can be concluded that the $c(2\times2)$ configuration obtained for Mn/Fe(001) survives when a Fe monolayer is added. It also survives when Oxygen is added. However while the $c(2\times2)$ configuration is the ground state for Mn/Fe(001) another configuration becomes more stable when a Fe monolayer is added and also for O/Fe/Mn/Fe(001).

After having determined the magnetic map for O/Fe/Mn/Fe(001) with the DFT-only approach we perform now calculations with the DFT+U approach. The reason to use DFT+U approach is twofold: 1) it has been shown by a great number of authors that such type of calculations when Oxygen is present should be used; 2) in a previous paper concerning O/Fe/Cr/Fe(001) [10] a drastic change in the interlayer exchange coupling was depicted when going from DFT-only approach to DFT + U. Therefore in this section the DFT + U approach is used to derive the magnetic map of O/Fe/Mn/Fe(001), the results are reported in Table 6. Similarly to the case of DFT approach we have considered seven input magnetic configurations displayed in Fig. 2. We have considered only the U=3.0 eV for the Fe atoms for the nearest neighbors of O surface atoms. The ground state is the b) input magnetic configuration. The magnetic moments, in the ground state are 0.17, 3.16 and -3.42 μ_B for the three first monolayers (O, Fe and Mn, respectively). The interlayer distances are 0.19, 1.82 and 1.43 Å for the three first monolayers (O, Fe and Mn, respectively).

A comparison can be made with the previous result concerning O/Fe/Cr/Fe(001)[10]. For O/Fe/Mn/Fe(001) as well as for O/Fe/Cr/Fe(001) the interlayer exchange coupling remains the same as the one depicted for Fe/Mn/Fe(001) and Fe/Cr/Fe(001), when DFT-approach is used. However, in the case of O/Fe/Cr/Fe(001) the interlayer exchange coupling is modified when the DFT + U approach is used. Similar result is obtained here for O/Fe/Mn/Fe(001). This modification of the IEC is linked to a drastic change of the LDOS on the Fe surface atom (see Fig. 4). This explanation is the same to that given by Meza-Aguilar and Demangeat [10] for O/Fe/Cr/Fe(001) described in a DFT + U scheme.

Recently, two of us[10] have discussed the stability of Fe/O/Cr/Fe(001) multilayers; within DFT and DFT + U code. It was clearly shown

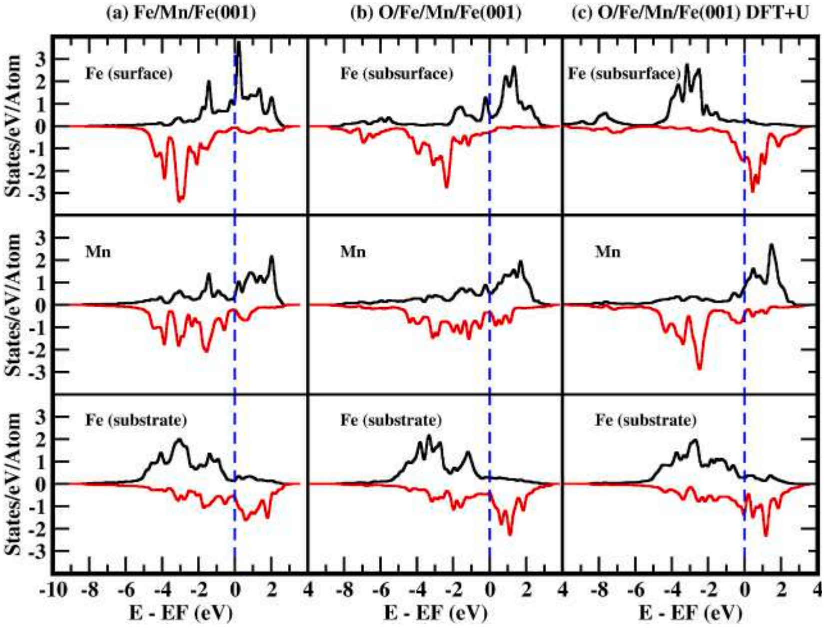

Fig. 4. Total local density of states for (a) Fe/Mn/Fe(001), (b) O/Fe/Mn/Fe(001) within DFT-only approach, and (c) O/Fe/Mn/Fe(001) using DFT+U. Only for the ground state is reported. The first line is for the Fe surface atom, the second line is for the Mn atom and finally the third line is for first monolayer of Fe substrate atom. The total density of state ($s+p+d$).

Table 5
Magnetic map and difference of total energy ΔE (in meV/atom), respectively to the ground state noted 0.0, for Fe/O/Mn/Fe(001) bcc. The ground state noted 0 is the ground state for O/Fe/Mn/Fe(001). The input magnetic configurations (IMC) are a), b), c), d), e), f) and g) are displayed in Fig. 2. The magnetic moments on Fe and Mn (in μ_B), the interlayer distance (d_I in Å) and total energy difference (in meV/atom) respect to the ground state noted by 0.0. Calculations are performed with DFT-code.

Fe/O/Mn/Fe(001)						
IMC ΔE	a) Non-Conv μ_B /d_I	b) 137 μ_B/d_I	c) 137 μ_B/d_I	d) Non-Conv μ_B/d_I	e) Non-Conv μ_B/d_I	f) Non-Conv μ_B/d_I
O		0.21/ 0.27	0.21/ 0.27			
O						
Fe		3.10/ 2.46	3.10/ 2.45			
Fe						
Mn		–3.69/ 1.44	–3.67/ 1.44			
Mn						
Fe_S		2.19/ 1.44	2.17/ 1.44			
Fe_S						
Fe_{S-1}		2.55/ 1.44	2.54/ 1.44			
Fe_{S-1}						
Fe_{S-2}		2.45/ 1.45	2.45/ 1.45			
Fe_{S-2}						

Table 6
Magnetic map and difference of total energy ΔE (in meV/atom), respectively to the ground state noted 0, for O/Fe/Mn/Fe(001) bcc. The input magnetic configurations (IMC) noted a), b), c), d), e), f) and g) are the same as those reported in Fig. 2. The magnetic moments on Fe and Mn (in μ_B), the interlayer distance (d_I in Å) and total energy difference (in meV/atom) respect to the ground state noted by 0.0. Calculations are performed with DFT + U code.

O/Fe/Mn/Fe(001)							
IMC ΔE	a) 117 μ_B /d_I	b) 0 μ_B/d_I	c) 108 μ_B/d_I	d) 152 μ_B/d_I	e) 88 μ_B/d_I	f) Non-Conv μ_B/d_I	g) 106 μ_B/d_I
O	0.21/ 0.41	0.17/ 0.19	0.23/ 0.47	–0.25/ 0.45	–0.23/ 0.41		0.00/ 0.37
O			0.20/ 0.24				–0.04/ 0.38
Fe	3.46/ 1.57	3.16/ 1.82	3.54/ 1.75	–3.58/ 1.62	–3.42/ 1.57		–3.52/ 1.64
Fe			3.54/ 1.75				3.52/ 1.66
Mn	1.55/ 1.36	–3.42/ 1.43	3.02/ 1.54	2.87/ 1.50	–2.08/ 1.41		–3.06/ 1.44
Mn			-3.48/ 1.44				2.12/ 1.44
Fe_S	1.68/ 1.41	2.15/ 1.42	2.13/ 1.41	2.42/ 1.43	2.50/ 1.45		2.14/ 1.42
Fe_S			2.13/ 1.41				2.12/ 1.42
Fe_{S-1}	2.42/ 1.46	2.54/ 1.44	2.56/ 1.50	2.39/ 1.45	2.51/ 1.43		2.54/ 1.45
Fe_{S-1}			2.55/ 1.46				2.52/ 1.47
Fe_{S-2}	2.44/ 1.44	2.46/ 1.46	2.55/ 1.46	2.45/ 1.44	2.45/ 1.45		2.52/ 1.46
Fe_{S-2}			2.55/ 1.46				2.52/ 1.46

Table 7
Magnetic map and difference of total energy ΔE (in meV/atom), respectively to the ground state noted 0, for Fe/O/Mn/Fe(001) bcc. The ground state noted 0.0 is the ground state for O/Fe/Mn/Fe(001). The input magnetic configurations (IMC) noted a), b), c), d), e), f) and g) are the same as those reported in Fig. 2. The magnetic moments on Fe and Mn (in μ_B), the interlayer distance (d_I in Å) and total energy difference (in meV/atom) respect to the ground state noted by 0. Calculations are performed with DFT + U code.

Fe/O/Mn/Fe(001)						
IMC ΔE	a) Non-Conv μ_B/d_I	b) 485 μ_B/d_I	c) Non-Conv μ_B/d_I	d) Non-Conv μ_B/d_I	e) 499 μ_B/d_I	f) Non-Conv μ_B/d_I
Fe		3.61/ 1.70			–3.62/ 1.61	
Fe						
O		0.00/ 1.09			–0.13/ 1.19	
O						
Mn		–4.62/ 1.97			–4.65/ 1.95	
Mn						
Fe_S		2.71/ 1.39			2.67/ 1.40	
Fe_S						
Fe_{S-1}		2.50/ 1.48			2.52/ 1.48	
Fe_{S-1}						
Fe_{S-2}		2.55/ 1.46			2.54/ 1.46	
Fe_{S-2}						

that those configurations are clearly unstable and that O atoms move above Fe surface. In this section we perform similar calculations. We start by discussing the DFT-only approach. In principle we had to perform calculations for all input magnetic configurations displayed in Fig. 2. We report on Table 5 the convergency for input magnetic configuration b and c clearly the "O" atoms move above the Fe surface atoms similarly to the case of Fe/O/Cr/Fe(001). Most probably, for the other input magnetic configurations the results will be the same. After having shown that for DFT approach the O atoms move above the Fe surface atoms we perform calculations within DFT + U approach.

Contrary to the result obtained in the DFT approach where O moves above the Fe surface atoms, now the converged solutions remain similar to the input one. The results for two specific input magnetic configuration b and e (see fig. 2 for definition) are reported in Table 7. It is shown that those converged solution are highly unstable as compared to the ground state b reported in Table 6. Let us point out that we can safely compare O/Fe/Mn/Fe(001) and Fe/O/Mn/Fe(001) because, in both cases the same number of O, respectively Mn and Fe atoms are concerned. Let us finally compare the results concerning Fe/O/Mn/Fe(001) with those of Fe/O/Cr/Fe(001). Similar results are obtained in both cases when the DFT-approach is used. However, in both cases, Fe/O/Cr/Fe(001) and Fe/O/Mn/Fe(001), the convergency moves the O atoms above the Fe surface. But, in both cases those solution were unstable when compared to the one with Oxygen on the surface.

We report the local density of states (LDOS) for the ground state for Fe surface atom in the system (a) Fe/Mn/Fe(001) and Fe subsurface atom in the system (b) O/Fe/Mn/Fe(001) using DFT+U, see Fig. 4. This switch of the IEC could be related to the drastic change of the local density of states (LDOS) on Fe atoms when we go from Fe/Mn/Fe(001) to O/Fe/Mn/Fe(001). Those LDOS are reported on Fig. 4 for the ground states of these two multilayered systems. Let us point out that these LDOS can be probed experimentally.

4. Conclusions

In a previous paper two of us [10] have shown that, for Fe/O/Cr/Fe

(001) the O atoms moves above the Fe surface atoms. Similar result is obtained here for Fe/O/Mn/Fe(001). Those results are experimentally sound. More specific in [10] was the fact that the interlayer exchange coupling changes sign when DFT + U approach is used instead of DFT. The purpose of the present communication was therefore to check if something similar happens for O/Fe/Mn/Fe(001).

Meza-Aguilar and Demangeat [10] have shown recently that the interlayer exchange coupling (IEC) of Fe/Cr/Fe(001) can be modified when an oxygen monolayer is added i.e. for O/Fe/Cr/Fe(001). This is clearly linked to a strong modification of the LDOS. In the present communication we see also a drastic modification of the LDOS when going from Fe/Mn/Fe(001) to O/Fe/Mn/Fe(001) when DFT + U is used. Consequently the IEC is modified.

Declaration of Competing Interest

The authors declare the following financial interests/personal relationships which may be considered as potential competing interests:

Salvador MEZA AGUILAR reports financial support and administrative support were provided by Universidad Autónoma de Sinaloa.

Acknowledgment

We acknowledge the support by the Universidad Autónoma de Sinaloa and SEP-CONACyT through Project PIFI 2005-25-06 UAS-ECFM, Project UAS-PROFAPI 2009/057, 2009/097, 2011/107, 2012/108, 2014/091, 2014/127, 2015/125, 2015/177, PRODEP-UAS-PTC-129 and CONACyT Project Number 99946. We acknowledge the computational resources provided by the Facultad de Ciencias Físico-Matemáticas de la Universidad Autónoma de Sinaloa, México. Calculations in this work have been done using the Quantum Espresso code[15].

References

[1] R.H. Aguilera-del Toro, F. Aguilera-Granja, M.B. Begaña, A. Vega, Phys. Chem. Chem. Phys. 23 (2021) 246.
[2] Y. Yonamoto, T. Yokoyama, K. Amemiya, D. Matsumura, T. Ohta, Phys. Rev. B 63 (2001) 214406.
[3] A. Tange, C. Gao, W. Wulfhekel, J. Kirschner, Phys. Rev. B 81 (2010) 220404.
[4] A. Picone, G. Fratesi, M. Riva, G. Bussetti, A. Calloni, A. Brambilla, M.I. Trioni, L. Duò, F. Ciccacci, M. Finazzi, Phys. Rev. B 87 (2013) 085403.
[5] A. Calloni, G. Fratesi, S. Achilli, G. Berti, G. Bussetti, A. Picone, A. Brambilla, P. Folegati, F. Ciccacci, L. Duò, Phys. Rev. B 96 (2017) 085427.
[6] C. Demangeat, J.C. Parlebas, Reports on Prog. in Phys. 65 (2002) 1679.
[7] A. Ernst, J. Henk, R.K. Thapa, J. Phys.: Cond. Matt. 17 (2005) 3269.
[8] H. Zenia, S. Bouarab, J. Ferrer, C. Demangeat, Surf. Sci. 564 (2004) 12.
[9] S. Pick, C. Demangeat, Surf. Sci. 584 (2005) 146–152.
[10] S. Meza-Aguilar, C. Demangeat, Eur. Phys. J. B 93 (2020) 107.
[11] P. Hohenberg, W. Kohn, Phys. Rev. 136 (1964) B864;
W. Kohn, L.J. Sham, Phys. Rev. 140 (1965) A1133.
[12] V.I. Anisimov, I.V. Solovyev, M.A. Korotin, M.T. Czyźyk, G.A. Sawatzky, Phys. Rev. B 48 (1993) 16929.
[13] A.I. Liechtenstein, V.I. Anisimov, J. Zaanen, Phys. Rev. B 52 (1995) R5467.
[14] S. Lany, Phys. Rev. B 87 (2013) 085112.
[15] P. Gianozzi, J. Phys.: Cond. Matt. 21 (2009) 395502.http://www.quantum-espresso.org
[16] J.P. Perdew, K. Burke, M. Ernzerhof, Phys. Rev. Lett. 77 (1996) 3865.
[17] The pseudopotentials without Spin-Orbit Coupling used are Fe.pbe-sp-van.UPF, Cr.pbe-sp-van.UPF and O.pbe-van_ak.UPF. These pseudopotentials were taken from Quantum Espresso Distribution: http://www.quantum-espresso.org.
[18] The ultrasoft pseudopotential of Vanderbilt is generated by the following address http://www.physics.rutgers.edu/~dhv/uspp/.
[19] M.A. Khan, J. Phys. Soc. Jpn 62 (1993) 1682.